ELSEVIER

Experimental studies on the onset of turbulence and frictional losses in an oscillatory turbulent pipe flow

T. S. Zhao and P. Cheng
Department of Mechanical Engineering, The Hong Kong University of Science and Technology, Clear Water Bay, Kowloon, Hong Kong

Transition to turbulence and frictional losses in an oscillatory and reversing flow of air in a pipe have been studied experimentally. A hot-wire anemometer was employed to observe temporal axial velocity variations, while a differential pressure transducer was used to measure temporal variations of pressure drops across the pipe. In contrast to previous work, the similarity parameters chosen for the present study are the kinetic Reynolds number Re_ω and the dimensionless oscillation amplitude of fluid A_o. A correlation equation in terms of these two similarity parameters for the prediction of the onset of turbulence is obtained. The experimental data show that a change from a favorable pressure gradient to an adverse pressure gradient at high kinetic Reynolds numbers and large dimensionless fluid displacements is responsible for the onset of turbulence. Based on the measured data of pressure drops and cross-sectional mean velocities, a correlation equation for the cycle-averaged friction coefficient of a cyclically turbulent oscillatory flow has been obtained in terms of the two similarity parameters.

Keywords: oscillatory flow; onset of turbulence; frictional losses

Introduction

Oscillating fluid flows are common physical phenomena frequently encountered in such engineering applications as internal combustion engines, Stirling engines, cryocoolers, and other periodical processes in thermal and chemical systems. Although the problem of oscillating flows has been studied for more than 100 years, a thorough understanding of the phenomena has not yet been achieved because of its complexity and the lack of experimental data. Richardson and Tyler (1929) were among the first to investigate experimentally an oscillatory flow in a pipe and discovered the so-called "annular effect"; i.e., the maximum velocity in an oscillatory flow occurs near the wall rather than at the center of the pipe, as in the case of unidirectional steady flow. Subsequently, a great deal of attention has been devoted to the study of transition to turbulence in an oscillatory flow. For example, Hino et al. (1976) studied transition by hot-wire measurements. Their measurements showed a laminar-like flow during the acceleration phase of the half cycle and a turbulent-like flow during the deceleration phase. A correlation equation for predicting the transition to turbulence was first given by Sergeev (1966), who used flow visualization to identify transition in an oscillating pipe flow. Ohmi et al. (1982) performed experiments on forced oscillations of a gas in a straight pipe. They found that velocity profiles during the laminar phase of cycle agree well with Uchida's (1950) analytical solution for a laminar fully developed oscillatory flow and that velocity profiles during the turbulent flow regime agree well with the 1/7th power-law of a steady turbulent pipe flow. They determined a correlation equation for the prediction of transition based on whether the observed velocity profiles are in agreement with the 1/7th power-law. Park and Bairti (1970) reported transition during free oscillations of a liquid in a U-tube. Iguchi et al. (1983) studied free oscillations in a U-tube experimentally and defined that transition occurred when the velocity profile deviated from Uchida-type laminar profiles. Using hot-wires, Seume (1988) experimentally studied the transition in an oscillatory pipe flow with the parameters range covered in the heat exchangers of Stirling engines and cryocoolers. Based on the streaming birefringence method, Kurzweg et al. (1989) observed the onset of turbulence in oscillating flow of water in small diameter tubes and found that with decreasing values of the Wommersley number, oscillatory flows become increasingly stable. Recently, Cooper et al. (1993) presented a review of literature on oscillating flows. However, none of the previous work has identified the physical reason for the onset of turbulence in an oscillatory and periodically reversing flow.

Recently, increasing attention has been given to the study of frictional losses in an oscillatory pipe flow because of its important applications to the design of heat exchangers in Stirling machines. For example, Roach and Bell (1989) performed an experiment on pressure drop in an oscillatory flow and found that pressure drop is independent of the frequency of oscillation. Wu et al. (1990) obtained some data for friction factor in a gap heat

Address reprint requests to Prof. P. Cheng, Department of Mechanical Engineering, The Hong Kong University of Science and Technology, ClearWater Bay, Kowloon, Hong Kong.

Received 16 May 1995; accepted 21 November 1995

Int. J. Heat and Fluid Flow 17: 356–362, 1996

655 Avenue of the Americas, New York, NY 10010

0142-727X/96/$15.00
PII S0142-727X(95)00108-5

exchanger and presented the data graphically as a function of the Reynolds number at given values of the oscillation frequency. Taylor and Aghili (1984) measured pressure drops in an oscillating flow of water in a pipe of a finite length at relatively low frequencies. Their data indicate an increase of the friction coefficient over an unidirectional steady flow. However, they did not have sufficient data to investigate the effects of frequency on the friction coefficient. More recently, Zhao and Cheng (1995a) obtained an analytical expression of the friction coefficient for a fully developed laminar oscillatory and reversing flow in a pipe and showed that this expression is in good agreement with their experimental data.

The objectives of the present work are: (1) to experimentally investigate the mechanisms of the transition to turbulence in a periodically oscillatory and reversing flow of air in a pipe; (2) to obtain a correlation equation in terms of appropriate similarity parameters for the onset of turbulence; and (3) to obtain a correlation equation for the cycle-averaged friction coefficient for a cyclically turbulent oscillatory flow in a pipe.

Governing equations and similarity parameters

Consider an incompressible flow in a pipe (with diameter D) whose oscillatory motion is driven by a sinusoidal displacer with the cross-sectional mean velocity u_m given by

$$u_m = u_{\max} \sin \phi \tag{1}$$

where the phase angle of the cross-sectional mean velocity ϕ, ranging from 0 to 360°, is related to the oscillation angular frequency ω and the time t by $\omega t = 2\pi(i-1) + \phi$, with i being the number of cycles. It should be pointed out that the maximum mean cross-sectional velocity $u_{\max}$ is related to the maximum fluid displacement $x_{\max}$ by

$$u_{\max} = \frac{x_{\max}\omega}{2} \tag{2}$$

If the dimensionless coordinates, time, velocity, pressure, and temperature are defined as $(X, R) = (x/D, r/D)$, $\tau = \omega t$, $U = u/u_{\max}$, $V = v/u_{\max}$, and $P = p/\rho u_{\max}^2$ (where x, r, t, p, u, and v are the corresponding dimensional quantities, and ρ is the density of the fluid), the governing dimensionless conservation equations of mass, and momentum for an incompressible periodically reversing flow are given by

$$\nabla \cdot \mathbf{V} = 0 \tag{3}$$

$$\mathrm{Re}_\omega \frac{\partial \mathbf{V}}{\partial \tau} + \mathrm{Re}_{\max}[\mathbf{V} \cdot \nabla \mathbf{V} + \nabla P] = \nabla^2 \mathbf{V} \tag{4}$$

where $\mathbf{V}$ denotes the velocity vector, $\mathrm{Re}_\omega = \omega D^2/\nu$ is the kinetic Reynolds number with ν being the kinematic viscosity of the fluid, and $\mathrm{Re}_{\max} = u_{\max} D/\nu$ is the Reynolds number. Thus, Seume (1988) used Re_ω and $\mathrm{Re}_{\max}$ as the similarity parameters to characterize an oscillatory and reversing flow in a pipe. Other investigators have used different similarity parameters. For example, Hino et al. (1976) used the Reynolds number $\mathrm{Re}_{\max}$ and the Stokes number λ as the similarity variables, where

$$\lambda = \frac{D}{2}\sqrt{\frac{\omega}{2\nu}} = \frac{1}{2}\sqrt{\frac{\mathrm{Re}_\omega}{2}}$$

Ohmi et al. (1982) used the Reynolds number $\mathrm{Re}_{\max}$ and the radius to viscous boundary thickness ratio Λ (where $\Lambda = R/\delta$ with $\delta = \sqrt{2\nu/\omega}$ being the Stokes layer thickness) as the similarity parameters. With the aid of Equation 2, it should be noted that the Reynolds number $\mathrm{Re}_{\max}$ is related to the frequency of oscillation by

$$\mathrm{Re}_{\max} = \frac{x_{\max}\omega D}{2\nu} \tag{5}$$

Thus, the similarity parameters Re_ω (or λ), $\mathrm{Re}_{\max}$, and Λ are all dependent on the oscillatory frequency. Although any two of these parameters can be used for the correlation of experimental data to characterize fluid dynamics aspects of an oscillatory and periodically reversing flow as was done in the previous studies, these choices of similarity parameter will not be able to isolate the effect of the oscillatory frequency. For this reason, another choice of parameters should be attempted for the correlation of

Notation

A_o	dimensionless oscillation of fluid defined in Equation 7
$\bar{c}_f$	cycle-averaged friction coefficient defined in Equation 13
$\bar{c}_{f,l}$	cycle-averaged friction coefficient of a laminar flow
$\bar{c}_{f,t}$	cycle-averaged friction coefficient of a turbulent flow
D	diameter of the pipe
Δp	pressure drop
L	length of the pipe
N	number of cycles to be ensemble-averaged
p, P	dimensional and dimensionless pressure of the fluid
r, R	dimensional and dimensionless radius of the pipe
Re_δ	Reynolds number based on the Stokes layer thickness δ
$\mathrm{Re}_{\max}$	Reynolds number based on the maximum cross-sectional mean velocity
Re_ω	kinetic Reynolds number
t, τ	dimensional and dimensionless time
τ_w	instantaneous wall shearing stress
$\bar{\tau}_w$	cycle-averaged wall shearing stress defined in Equation 12
u, U	dimensional and dimensionless axial velocity
u_m	dimensional cross-sectional mean velocity
$u_{\max}$	dimensional maximum cross-sectional mean velocity
v, V	dimensional and dimensionless radial velocity
$\mathbf{V}$	velocity vector
x, X	dimensional and dimensionless axial distance
$x_{\max}$	dimensional maximum fluid displacement

Greek

δ	Stokes layer thickness
λ	Stokes number
Λ	ratio of the radius to the viscous boundary-layer thickness
ν	kinematic viscosity of fluid
ρ	density of fluid
ϕ	phase angle
ω	angular frequency
Ω	period of oscillation

Subscripts

m	cross-sectional mean value
max	maximum value
o	oscillation
w	wall

experimental data. To this end, it should be noted that Equation 5 can be rewritten as

$$\mathrm{Re}_{\max} = \frac{A_o}{2}\,\mathrm{Re}_\omega \tag{6}$$

where

$$A_o = \frac{x_{\max}}{D} \tag{7}$$

is the dimensionless oscillation amplitude of fluid. Substituting Equation 6 into Equation 4 yields

$$\frac{\partial \mathbf{V}}{\partial \tau} + \frac{A_o}{2}[(\mathbf{V}\cdot\nabla)\mathbf{V} + \nabla P] = \frac{1}{\mathrm{Re}_\omega}\nabla^2\mathbf{V} \tag{8}$$

which shows that for a given dimensionless oscillation amplitude of fluid A_o, the kinetic Reynolds number Re_ω in an oscillatory flow plays the same role as that of the Reynolds number in a unidirectional flow, which describes the relative importance of the inertial force and the frictional force. Equations 3 and 8 show that A_o and Re_ω are the two alternatives similarity parameters for an incompressible periodically reversing flow. Because the amplitude of fluid displacement and the oscillatory frequency are independent of each other, this choice of similarity parameters for the correlation of experimental data will be able to indicate the effects of amplitude of fluid displacement and oscillatory frequency separately.

Experimental apparatus

The experiment was performed using the test rig shown in Figure 1. The oscillating motion of flow was induced by a piston moving sinusoidally inside a cylinder. The piston was driven by a 1 kW DC motor with an adjustable speed from 0.12 to 10 Hz. The working fluid (air) moved reversibly and periodically in the test section, which was made of a long copper tube, $D = 1.35$ cm in diameter and $70D$ in length. At the two ends of the test section, two velocity straightening chambers (made of fine screens) were connected to ensure a uniform flow entering the test section. The test section was connected at two ends of the pump by flexible tubes.

A differential pressure transducer (Validyne Model DP15), having a high natural frequency (> 5000 Hz), was used to measure pressure drop in the pipe. To avoid or minimize the entrance effect and to measure the pressure drop in the fully developed flow region, each differential pressure transducer tap was installed at a distance of $10D$ from each end of the pipe (shown in Figure 1). For the maximum fluid flow displacement $A_o = 113.51$ of the present experiment, the entrance length L_e was $9.42D$, which was evaluated using $L_e/D = 0.081\,A_o + 0.23$ provided by Zhao and Cheng (1995b). Therefore, the pressure transducer taps were located in the fully developed flow region in this study. A miniature straight hot-film probe (TSI, Model 1260A-10) with a manual traverse mechanism was installed at the middle section of the pipe for measurements of the instantaneous axial velocity at different radial positions. Analog-to-digital conversions were carried out by a conversion board (MetraByte, DAs-20), which was plugged in a 486 personal computer. A 4-channel simultaneous sample and hold front end for the A/D board (MetraByte, SSH-4) was employed so that both pressure and velocity voltage signals could be sampled simultaneously. An digital oscilloscope (Phillips, Model PM 3335) was also used to observe velocity and pressure signals simultaneously. An angle shaft encoder (Lucas Ledex, Model LD23) was mounted on the crank shaft to provide top dead center signals and sampling intervals for each cycle.

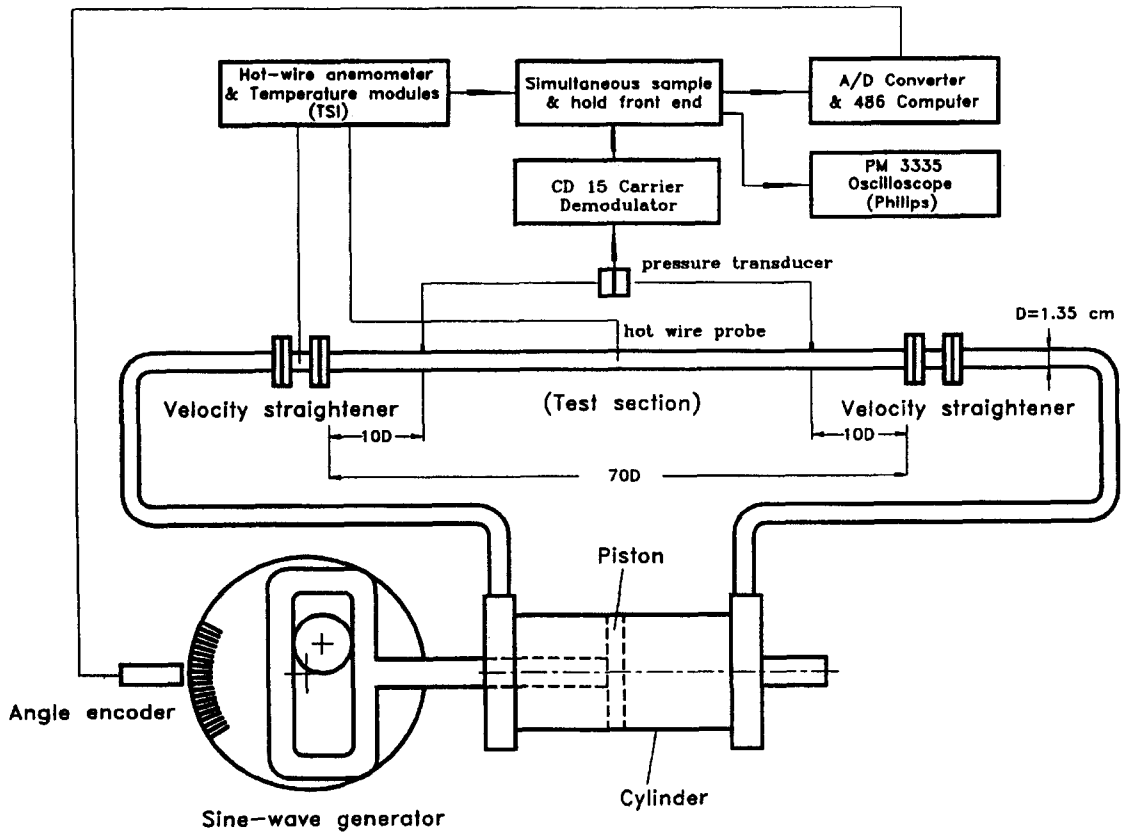

Figure 1 Schematic diagram of experimental apparatus

An uncertainty analysis based on the method described by Moffat (1988) was performed. Uncertainty in the kinetic Reynolds number Re_ω was dominated by the measurement of oscillation frequencies and was estimated at 2.3%. Uncertainty in the dimensionless oscillation amplitude of the fluid A_o was computed to be less than 0.5%, which was primarily influenced by errors in measuring the stroke and the diameter of the air pump. The main source of errors in the reported results on the friction coefficient is statistical uncertainty in the ensemble-averaged quantities of velocities and pressure drops due to the finite number of measurements. The statistical uncertainty in the ensemble-averaged velocity is estimated to be 2.5%, assuming uncorrelated, normally distributed measurements with a 95% confidence level. Similarly, the statistical uncertainty in the ensemble-averaged pressure drop varies from 5 to 10%. The largest uncertainties in the measured cycle-averaged friction coefficient $\bar{c}_{f,\exp}$ were computed to be about 13%.

Results and discussion

Onset of turbulence

Instantaneous axial velocity variations at different radial positions were sampled at the middle section of the pipe for different values of the dimensionless oscillation amplitude of fluid A_o and the kinetic Reynolds number Re_ω. Because the hot-wire anemometer cannot detect the direction of the fluid flow, all values of the velocity are presented as absolute values. Typical velocity traces in the laminar flow regime, transition, and turbulent flow regime are illustrated from Figures 2 to 5. Measurement results of the onset of the turbulence are presented in Figure 6.

Experiments were first conducted for an oscillatory flow at low dimensionless oscillation amplitudes of fluid and low kinetic Reynolds numbers. Figures 2a and 2b illustrate typical temporal velocity variations at different radial positions for $A_o = 57.5$ and $Re_\omega = 66.6$, as well as for $A_o = 21.4$ and $Re_\omega = 302$, respectively. At these small values of A_o and Re_ω, it is shown that variations of the axial velocity are smooth, indicating that the flow is laminar everywhere. It is also noted that axial velocities at different radial positions vary sinusoidally with time, with axial velocities in the core having a slight phase delay with respect to those near the wall.

When the values of A_o and Re_ω were increased to certain values, it was observed from the oscilloscope that periodic turbulent bursts occurred near the wall during certain times of the cycle. Figures 3a and 3b show two examples of temporal axial velocity variations at the pipe centerline and near the wall at the onset of turbulence. It should be noted from these figures that the velocity fluctuations near the wall are much stronger than in the centerline of the pipe. This finding implies that the instabilities were generated near the wall and the radial momentum transfer caused a lower level of velocity fluctuations near the centerline. This is because at high kinetic Reynolds numbers the annular effect becomes pronounced and there exist inflexion points in the velocity profile near the wall. Thus, at a critical value of the kinetic Reynolds number, the fluid flow near the wall may first become unstable and eddies occur near the wall. These eddies are transferred to the core flow, which causes small fluctuations. As observed by previous investigators, we found that turbulence disappeared and the flow recovered to a laminar-like flow in the accelerating period of the half cycle for which a favorable pressure gradient exists.

Figure 4 illustrates an example of a fully turbulent flow at $A_o = 97.1$ and $Re_\omega = 302.2$. It is shown that axial velocity fluctuations become much more significant both near the wall and in the core flow. It is interesting to compare Figure 3a with Figure 4, where the dimensionless oscillation amplitude of fluid is fixed

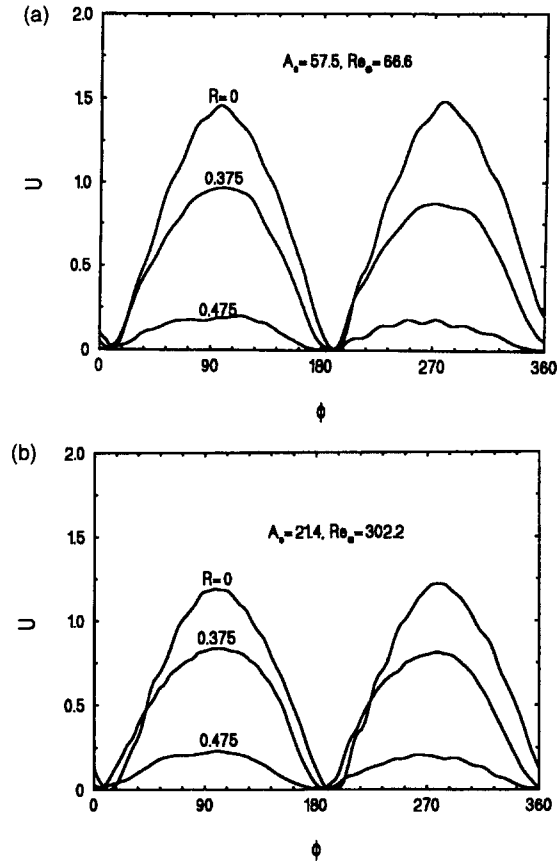

Figure 2 (a) Temporal axial velocity variations of a laminar flow for $A_o = 57.5$ and $Re_\omega = 66.6$; (b) Temporal axial velocity variations of a laminar flow for $A_o = 21.4$ and $Re_\omega = 302.2$.

at $A_o = 97.1$, while the kinetic Reynolds number is increased from $Re_\omega = 66.6$ to 302.2. It is apparent that the velocity fluctuations near the wall at a high kinetic Reynolds number are much larger than those at a low kinetic Reynolds number. Similarly, when comparing Figures 3b and 4 where the kinetic Reynolds number is fixed at $Re_\omega = 302.2$, while the dimensionless oscillation amplitude is increased from $A_o = 47.1$ to 97.1, we found that velocity fluctuations become larger with the increase of A_o.

Figures 5a and 5b show temporal variations of the pressure gradient and the axial velocity near the wall of the pipe under the same conditions as those of Figures 3a and 3b. The axial velocity and pressure signals were sampled simultaneously. It is shown that the flow is laminar during the acceleration period for which a favorable pressure gradient exists in the flow direction. However, during the beginning of the deceleration period and at the instance for which the favorable pressure gradient changes to an adversed pressure gradient, large velocity fluctuations occurs. As the magnitude of the velocity becomes sufficiently small, velocity fluctuations subside and the flow relaminarizes again. This observation suggests that the change from a favorable pressure gradient to an adversed pressure gradient is responsible for the onset of turbulence at sufficiently high kinetic Reynolds numbers and sufficiently large dimensionless fluid displacements. The physical mechanism leading to the onset of turbulence is a complicated interaction of the inertial force, viscous force, and pressure gradient effects that can be explained as follows. At sufficiently high kinetic Reynolds numbers and large fluid displacements, the interaction of the inertia and viscous force leads to annular velocity profiles for which inflexion points exist near the wall. At the instance when the pressure gradient changes from a favorable

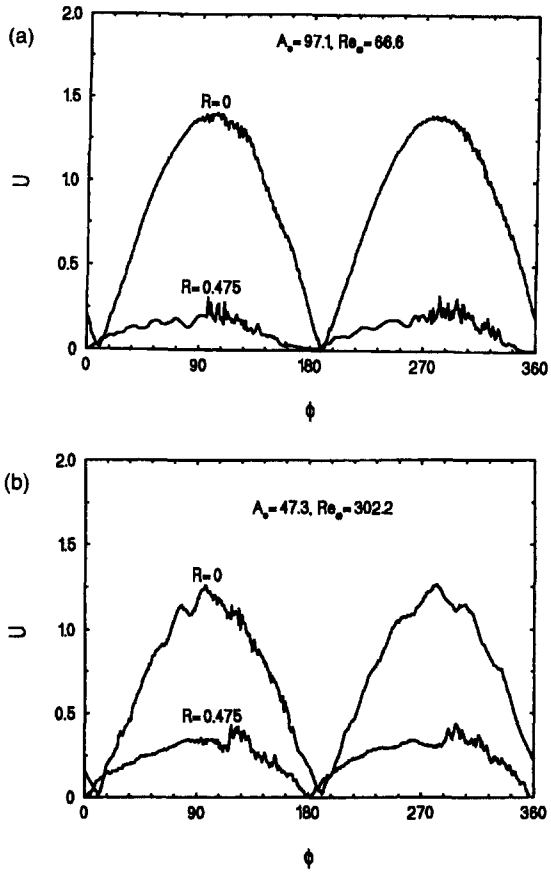

Figure 3 (a) Temporal axial velocity variations at the onset of transition to turbulence: $A_o = 97$ and $Re_\omega = 66.6$; (b) Temporal axial velocity variations at the onset of transition to turbulence: $A_o = 47.3$ and $Re_\omega = 302.2$

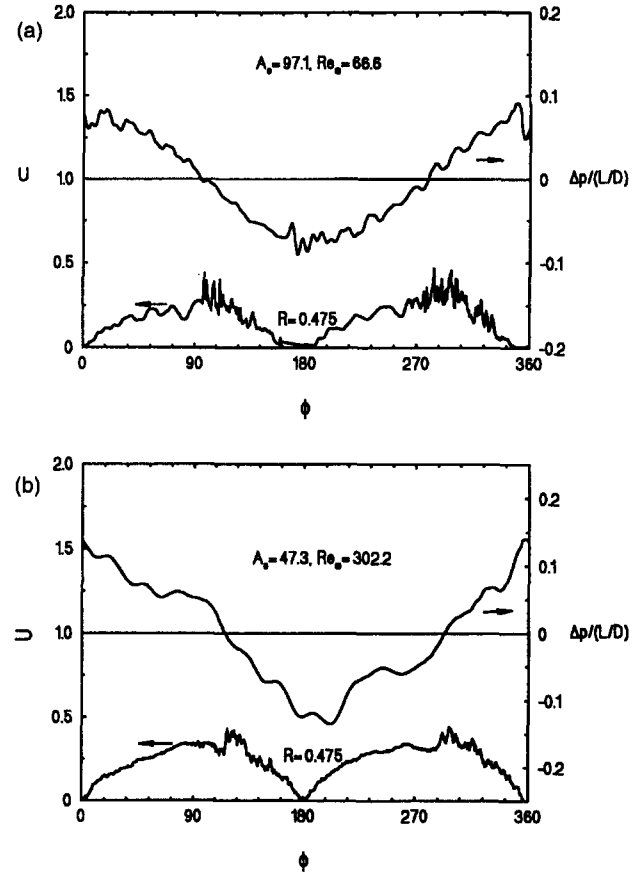

Figure 5 (a) Temporal variations of axial velocity and pressure drop at the onset of transition to turbulence: $A_o = 97.1$ and $Re_\omega = 66.6$; (b) Temporal variations of axial velocity and pressure drop at the onset of transition to turbulence: $A_o = 47.3$ and $Re_\omega = 302.2$

to an adversed condition, the simultaneously existence of large velocity magnitude and the inflexion points in the velocity profiles as well as the adversed pressure gradient leads to the onset of instability. During the end of the deceleration period, the magnitude of velocity is small, and the flow relaminarizes again although the inflexion points still exist in the velocity profiles.

In the present investigation, the onset of turbulence was designated as soon as significant velocity fluctuations appeared in the oscilloscope at the end of acceleration period or at the beginning of deceleration period as previously shown in Figures 3a and 3b. To identify the onset of turbulence, experiments were carried out first for small dimensionless oscillation amplitudes and low kinetic Reynolds numbers. At a given dimensionless oscillation amplitude of fluid A_o, the value of the kinetic Reynolds number Re_ω was gradually increased until the onset of turbulence, as observed on the screen of the oscilloscope. We then recorded the critical value of the kinetic Reynolds number at each dimensionless oscillation amplitude of fluid. It is found that the data for the onset of turbulence, as represented by solid circles in Figure 6, are well fitted by the following algebraic expression:

$$(A_o)_{cri} = \frac{761}{\sqrt{(Re_\omega)_{cri}}} \tag{9a}$$

or

$$\sqrt{2}\,(Re_\delta)_{cri} = A_o\sqrt{Re_\omega} = x_{max}\sqrt{\frac{\omega}{\nu}} = 761 \tag{9b}$$

where $(Re_\delta)_{cri}$ is the Reynolds number based on the Stokes layer thickness δ. The parameter Re_δ is the critical transition parameter identified by Sergreev (1966) and Kurzweg et al. (1989). Note that Equation 9a was obtained based on experimental data in the ranges of $8.05 \le A_o \le 121.1$ and $23 \le Re_\omega \le 540$. Kurzweg et al. found some experimental evidence that the critical value of

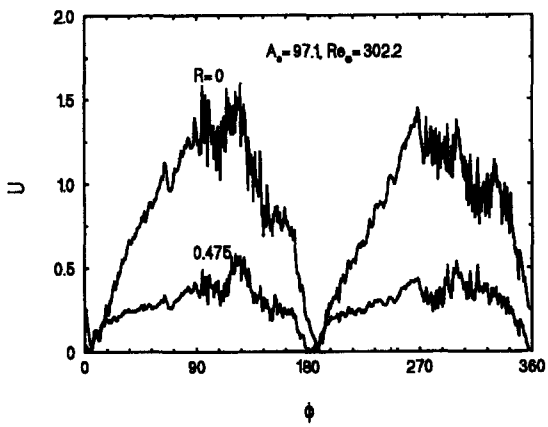

Figure 4 Temporal axial velocity variations of a turbulent flow for $A_o = 97.1$ and $Re_\omega = 302.2$

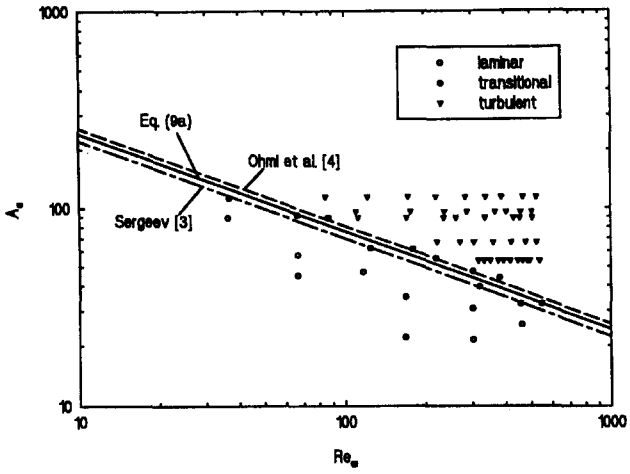

Figure 6 Correlation equation of the critical dimensionless oscillation amplitude of fluid A_o and the kinetic Reynolds number Re_ω

$(Re_\delta)_{cri}$ depends on Re_ω at very small values of A_o and Re_ω. Equation 9a is presented as a solid straight line in Figure 6, where laminar and turbulent flows exist below and above this line. As shown in Figure 6, the onset of the turbulence in an oscillatory pipe flow occurs at high dimensionless oscillation amplitudes of fluid and high kinetic Reynolds numbers; the critical value of A_o decreases with the increase of Re_ω. It is interesting to see that the present measurement is quite closed to the data obtained by Sergeev (1966) and Ohmi et al. (1982), represented by the dotted line and the dashed lines, respectively, in Figure 6. The slight discrepancies can be attributed to the different criteria or measurement methods employed. Ohmi et al. determined the correlation equation for the prediction of transition based on whether the observed velocity profiles are in agreement with the 1/7th power-law. Sergeev used aluminum particle flow visualization but did not state his criterion. It should be noted that the effect of the hot-wire probe's wake may be present with the present measurements. On this point, Merkli and Thomann (1975) found that the disturbances of the flow induced by the hot-wire probe become significant only when the frequencies are higher than 85 Hz, while the disturbances vanish under lower frequencies. The present measurements were carried out for frequencies less than 10 Hz.

Frictional losses in a cyclically turbulent flow

To obtain a correlation equation for the pressure drop in a fully developed oscillatory flow, consider the following unsteady momentum integral equation:

$$\frac{\Delta p}{L} = \rho \frac{du_m}{dt} + \frac{4\tau_w}{D} \tag{10}$$

where u_m is the cross-sectional mean velocity, and τ_w is the wall shearing stress that is valid for both laminar and turbulent flow. Solving for τ_w from Equation 10 yields

$$\tau_w = \frac{1}{4}\left(\Delta p \frac{D}{L} - \rho D \frac{du_m}{dt}\right) \tag{11}$$

Because the wall shearing stress is a time-resolved quantity that can be both positive or negative during one cycle, the cycle-averaged wall shearing stress $\bar{\tau}_w$ based on the absolute values of instantaneous wall shearing stress τ_w is defined as follows:

$$\bar{\tau}_w = \frac{1}{\Omega}\int_0^\Omega |\tau_w(t)|\,dt \tag{12}$$

where $\Omega = 2\pi/\omega$ is the period of oscillation. The corresponding cycle-averaged friction coefficient $\bar{c}_f$ is defined as follows:

$$\bar{c}_f = \frac{\bar{\tau}_w}{\frac{1}{2}\rho u_{max}^2} \tag{13}$$

Substituting Equation 11 in Equations 12 and 13 yields

$$\bar{c}_f = \frac{1}{2\rho u_{max}^2}\frac{1}{\Omega}\int_0^\Omega \sqrt{\left(\Delta p \frac{D}{L} - \rho D \frac{du_m}{dt}\right)^2}\,dt \tag{14}$$

where Δp and u_m were measured by a differential pressure transducer and a hot-wire anemometer, respectively. In this study, the ensemble-averaged pressure drop and the ensemble-averaged axial cross-sectional mean velocity were used to compute the cycle-averaged friction coefficient given by Equation 14. The number of the samples to be ensembly averaged is 100 cycles.

In a recent paper by Zhao and Cheng (1995a), the friction coefficient of a fully developed laminar oscillatory flow $\bar{c}_{f,l}$ in a pipe was investigated theoretically and experimentally. They proposed and experimentally verified the following approximated correlation equation for the prediction of the cycle-averaged friction coefficient in the laminar flow regime:

$$\bar{c}_{f,l} = \frac{3.27192}{A_o\left(Re_\omega^{0.548} - 2.03946\right)} \tag{15}$$

which is valid in the range of $23 \le Re_\omega \le 395$ and $0 \le A_o \le 26.4$.

The friction coefficient of a cyclically turbulent oscillatory flow $\bar{c}_{f,t}$ was measured in the present study. The range of the dimensionless oscillation amplitude of the fluid A_o and the kinetic Reynolds number Re_ω covered in this study is illustrated in Figure 6. Forty-three experimental runs, represented by triangle symbols above the solid line in Figure 6, were performed to obtain the friction coefficient in the turbulent flow regime. The measured data are shown in Figure 7, where the cycle-averaged friction coefficient multiplied by the dimensionless oscillation amplitude of the fluid A_o is plotted against the kinetic Reynolds number Re_ω. It was found that the following algebraic equation fits with the measured data with a maximum error of 14.8%:

$$\bar{c}_{f,t} = \frac{1}{A_o}\left(\frac{76.6}{Re_\omega^{1.2}} + 0.40624\right) \tag{16}$$

which is valid in the range of $81 \le Re_\omega \le 540$ and $53.4 \le A_o \le 113.5$. For comparison, the correlation equation of the cycle-aver-

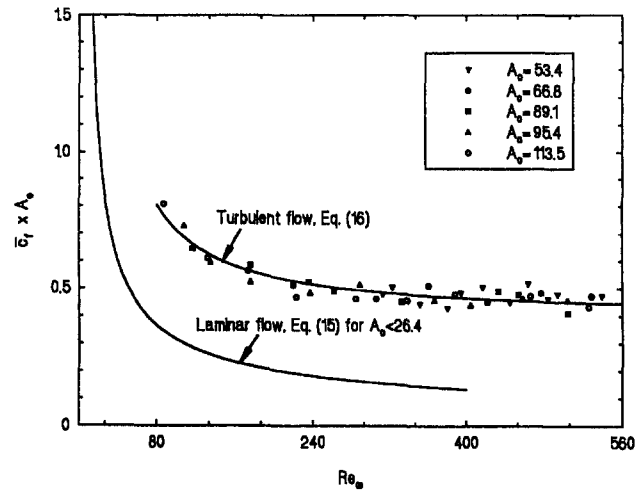

Figure 7 Correlation equations of the cycle-averaged friction coefficient in terms of A_o and Re_ω for oscillatory flow

aged friction coefficient for the laminar flow given by Equation 15 is also presented in Figure 7. It is evident that the value of $\bar{c}_f A_o$ for a turbulent flow is significantly higher than that of a laminar flow at the same kinetic Reynolds number.

Concluding remarks

The onset of turbulence and frictional losses in a cyclically turbulent oscillatory flow in a pipe have been investigated experimentally. As in the previous investigations, it is found that onset of turbulence occurs only in the deceleration period of the half cycle. It has been shown that a change from a favorable pressure gradient to an adverse pressure gradient at high kinetic Reynolds numbers and large dimensionless fluid displacements is responsible for the onset of turbulence during a cycle in an oscillatory and reversing pipe flow. The kinetic Reynolds number and the dimensionless fluid displacement are identified as the two independent similarity parameters for the problem under consideration. A correlation equation in terms of these two similarity parameters for the onset of turbulence is obtained. Based on the measured data of pressure drops and cross-sectional mean velocities, a correlation equation for the cycle-averaged friction coefficient of a cyclically turbulent flow has been obtained, which is valid in ranges of $81 \leq \mathrm{Re}_\omega \leq 540$ and $53.4 \leq A_o \leq 113.5$. A comparison of the cycle-average friction coefficient for the turbulent flow and laminar flow is made. These correlation equations are useful in the design of heat exchangers in a Stirling machine and pulse tubes in a cryocooler.

References

Cooper, W. L., Yang, K. T. and Nee, V. W. 1993. Fluid mechanics of oscillatory and modulated flows and associated applications in heat and mass transfer — A review. *J. Energy, Heat, Mass Transfer*, **15**, 1–19

Hino, M., Sawamoto, M. and Takasu, S. 1976. Experiments on the transition to turbulence in an oscillating pipe flow. *J. Fluid Mech.* **75**, 193–207

Iguchi, M., Ohmi, M. and Maegawa, K. 1983. Analysis of free oscillating flow in a U-shaped tube. *Bull. JSME*, **25**, 1398–1405

Kurzweg, U. H., Lindgren, E. R. and Lothrop, B. 1989. Onset of turbulence in oscillating flow at low Womersley number. *Phys. Fluids A*, **1**, 1912–1915

Merkli, P. and Thomann, H. 1975. Transition to turbulence in oscillating pipe flow. *J. Fluid Mech.*, **68** 567–575

Moffat, R. J. 1988. Describing the uncertainties in experimental results. *Exp. Thermal Fluid Sci.* **1**, 3–17

Ohmi, M., Iguchi, M. and Urahata, I. 1982. Flow patterns and frictional losses in an oscillating pipe flow. *Bull. JSME*, **25**, 536–543

Park, J. and Baird, M. 1970. Transition to turbulence in an oscillating manometer. *Can. J. Chem. Eng.* **48**, 491–495

Richardson, E. G. and Tyler, E. 1929. The transverse velocity gradient near the mouths of pipes in which an alternating or continuous flow of air is established. *Proc. Phys. Soc. London*, **42**, 1–15

Roach, P. D. and Bell, K. J. 1989. Analysis of pressure drop and heat transfer data from the reversing flow test facility. Report # ANL/MCT-88-2, Argonne National Laboratory, Argonne, IL

Sergreev, S. 1966. Fluid oscillations at moderate Reynolds numbers. *Fluid Dynamics*, **1**, 121–122

Seume, J. R. 1988. An experimental investigation of transition in an oscillating pipe flow. Ph. D. diss. University of Minnesota, Minneapolis, MN

Taylor, D. R. and Aghili, H. 1984. An investigation of oscillating flow in tubes. *Proc. 19th Intersociety Energy Conversion Engineering Conference* (IECEC Paper 84916), pp. 2033–2036, American Nuclear Society

Uchida, S. 1950. The pulsating viscous flow superposed on the steady laminar motion of an incompressible fluid in a circular pipe. *ZAMP*, **7**, 403–422

Wu, P., Lin, B., Zhu, S., He, Y., Ren, C. and Wang, F. 1990. Investigation of oscillating flow resistance and heat transfer in the gap used for cryocoolers. *Proc. 13th Intersociety Energy Conversion Engineering, Conference*

Zhao, T.S. and Cheng, P. 1995a. The friction coefficient of a fully developed laminar reciprocating flow in a circular pipe. *Int. J. Heat and Fluid Flow*, **17**, 167–172

Zhao, T.S. and Cheng, P. 1995b. Hydrodynamically developing laminar oscillatory flow in a circular pipe. Submitted for publication